Astrometric and photometric measurements of GEO satellites in proximity operations over the Pacific

Jovan Skuljan
Defence Technology Agency, Auckland, New Zealand

ABSTRACT

A large number of observations of geostationary satellites in proximity operations were collected in February 2020 from New Zealand. The measurements were part of the "Phantom Echoes" experiment, a collaborative activity between Australia, Canada, New Zealand, the United Kingdom and the United States. As a suitable case study, the docking between the Mission Extension Vehicle-1 (MEV-1) and Intelsat 901 was selected. During the final part of the proximity operation, the two satellites were positioned over the Pacific Ocean and therefore visible from New Zealand.

The observations were made from the Defence Technology Agency's (DTA) Space Domain Awareness (SDA) Observatory on Whangaparaoa Peninsula north of Auckland. All images were taken with an 11-inch (279 mm) Celestron Edge HD telescope, equipped with a FLI ML11002 CCD camera. The DTA observatory has recently been fully automated, allowing for continuous data collection throughout the night. Up to 1500 images were routinely collected on every clear night, using a sampling rate of about 3 frames per minute (180 per hour) for increased time resolution both in photometry and astrometry. The apparent magnitude limit for satellite detection was about 15, based on the exposure time of 5 seconds. In practice, the results were only acceptable when the objects were at around magnitude 14, or brighter.

The data reductions were performed in StarView, a dedicated software tool developed at DTA for SDA image analysis. A specially developed data analysis algorithm was used for the astrometric calibration of both stellar (sidereal) images and satellite (non-sidereal) images. A typical RMS error of the astrometric solution was 0.2 arc seconds, based on about 100-400 stars identified in the field of view. The European Space Agency's GAIA catalogue (DR2), limited down to magnitude 16, was used for the calibration. The random measurement errors in relative astrometry between the two satellites was typically less than 0.1 arcsec, corresponding to less than 20 m in space. A typical photometric calibration based on the GAIA G-band produced an RMS error of about 0.1 – 0.2 magnitudes. At the same time, the random errors in aperture photometry were only between about 0.02 and 0.04 in good atmospheric conditions.

Using the high-quality measurements obtained during the proximity operations of MEV-1 and Intelsat 901 it was possible to correlate certain characteristic features in the observed astrometric and photometric data with the actual manoeuvres and other key events performed during the mission. It was demonstrated that readily available small-aperture optical equipment can successfully be used to monitor proximity operations in Earth geostationary orbit (GEO) and collect important information for space domain awareness.

1. INTRODUCTION

This work is part of the "Phantom Echoes" experiment [1] – a collaborative effort between Australia, Canada, New Zealand, the United Kingdom and the United States in the field of space domain awareness (SDA) with the aim of examining rendezvous and proximity operations in the Earth geostationary orbit (GEO). The observation campaign was focused on the Mission Extension Vehicle-1 (MEV-1, NORAD 44625), a commercial satellite built by Northrop Grumman, launched in October 2019, and successfully docked to Intelsat 901 (NORAD 26824) in February 2020. Prior to the docking, both satellites were moved to a super synchronous graveyard orbit, causing them to slowly drift westwards during the final weeks of the operation. The docking was originally planned for late January, or early February, while the two satellites were still positioned above the eastern Pacific Ocean, but due to a number of factors, the operation was postponed, and the actual docking was completed on 25th February 2020 at 7:15 UTC over the Western Pacific. During the entire month of February, the satellites were well positioned for observations from New Zealand, starting at an altitude of about 33 degrees above the north-eastern horizon early in

the month, reaching 46 degrees around the meridian in mid-February, and finishing at 30 degrees above the north-western horizon towards the end of the month.

2. OBSERVATIONS

All observations were made from the Defence Technology Agency's (DTA) SDA Observatory (36° 36′ 08.5″ S, 174° 50′ 05.6″ E) located on Whangaparaoa Peninsula, just north of Auckland, New Zealand. The observatory is fully automated and equipped with two 11-inch (279-mm) telescopes: an EdgeHD f/10 Cassegrain and a RASA f/2.2 astrograph. Only the f/10 Cassegrain (2800 mm focal length) was used for the observations described in this paper. An FLI ML11002 full-frame CCD camera was used as a detector. This camera provides a diagonal field of view of almost one degree and a pixel scale of 0.66 arc seconds per pixel.

A total of over 11,000 images were collected over 11 nights of observation, as summarized in Table 1. Typical exposure duration was 5 seconds, followed by 15 seconds of idle time between exposures. In average, this produced three frames per minute or 180 frames per hour, which is a somewhat higher frame rate than normally used with GEO targets. However, the aim was to increase the time resolution in order to detect any small changes in astrometry and photometry during the final stages of the MEV-1 operation.

Table 1. List of observations of MEV-1 and Intelsat 901 from New Zealand during February 2020.

UTC Date	*UTC Start*	*UTC Finish*	*Total hours*	*Total frames*
2020-Feb-05	10:06:28	15:56:34	5.8	1334
2020-Feb-11	09:58:03	17:00:48	7.0	789
2020-Feb-12	08:23:27	15:57:17	7.6	847
2020-Feb-13	10:04:01	17:18:33	7.2	1483
2020-Feb-14	09:01:15	10:12:37	1.2	134
2020-Feb-17	09:58:12	17:23:37	7.4	831
2020-Feb-19	08:15:35	14:47:47	6.5	732
2020-Feb-20	07:56:35	13:44:55	5.8	643
2020-Feb-23	09:00:55	17:10:50	8.2	1319
2020-Feb-24	08:11:43	17:27:10	9.3	1503
2020-Feb-25	08:12:51	17:24:27	9.2	1494

An illustration of the final approach between MEV-1 and Intelsat 901 on 24th February 2020 is shown in Fig. 1. The sequence starts at 13:30 UTC, when the two satellites were about 9 arc seconds apart. The apparent magnitude of Intelsat 901 at this time was 10.3^{m}, while MEV-1 appeared much fainter at 12.9^{m}.

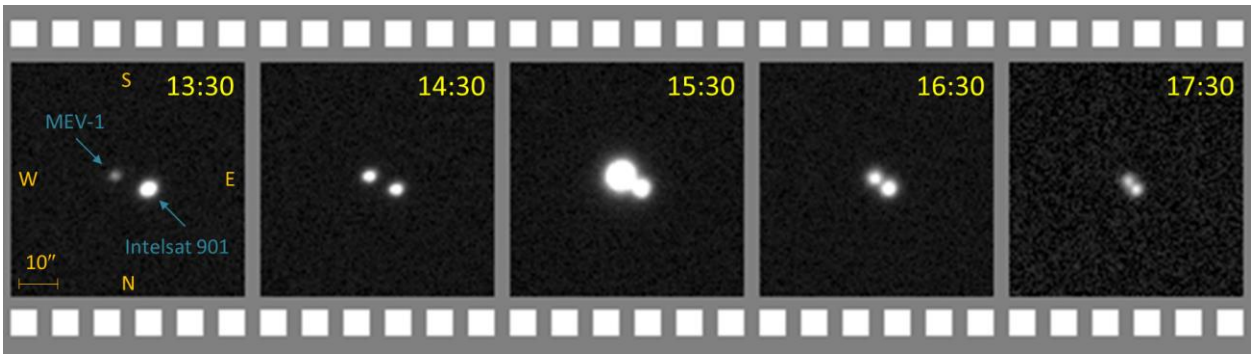

Fig. 1. The final approach of MEV-1 and Intelsat 901, recorded on 24th February 2020. Each frame has a field of view of 60 × 60 arc seconds. All times are in UTC.

One hour later, at 14:30 UTC, the separation was about 7.5 arcsec and both satellites were at about the same magnitude of 11.3. Later during the night, the satellites passed through the Earth's shadow and therefore were not visible, between 15:00 and 15:20. After the eclipse, at 15:30 UTC, MEV-1 was much brighter (magnitude 7.9), while the separation was reduced to about 6 arcsec. This was further reduced to 4.3 arcsec at 16:30. The final frame was taken at 17:30, when the sky was already getting brighter and the photon noise in the background started to increase. The two satellites were recorded at a separation of 2.8 arcsec, equivalent to about 500 m in space at the range of 39,000 km. This was the last image of the pair before the docking that took place during NZ daylight on the same day.

3. DATA REDUCTION

All data reductions were performed in StarView, a dedicated SDA data analysis tool developed at DTA [2, 3, 4]. The software uses the European Space Agency's GAIA catalogue data release 2 [5, 6] for both astrometric and photometric calibrations. A subset of GAIA stars down to magnitude 16 (a total of 77.3 million objects) has been used for faster processing and lower demand on computing resources.

Initial astrometric and photometric calibration was performed for each observation night on a stellar field taken in sidereal mode and close to the region where the satellite observations will be collected. The exposure duration was typically 10 seconds, for improved signal-to-noise ratio. A typical stellar field contained between about 100 and 1000 stars depending on the sky region (i.e. how far from the Milky Way the camera is pointed). A preliminary identification of the region was performed in StarView using a novel algorithm called "stellar fingerprints" [2]. The algorithm was developed at DTA, and provides a very reliable method for fast identification of stellar fields by extracting a small subset (10 – 50) of "reference" stars around the centre of the image. The remaining stars in the field were identified in an iterative process using standard two-dimensional polynomial regression, where new stars were added to the solution one at a time, based on the distance from the centre of the reference cluster. At the same time, the polynomial degree was increased gradually, as the number of stars increased. A satisfactory solution is usually obtained using a maximum degree of 3. This approach gives very good results in terms of stability and quality of the final solution. The random uncertainty (RMS error) of the polynomial fit typically stays well below one pixel, which corresponds to a fraction of arc second. A good astrometric solution gives an RMS error between 0.1 and 0.2 arcsec. Usually, there is a very small difference between the uncertainties in right ascension and declination, as the stellar profile (PSF function) often exhibits a slight asymmetry in X and Y directions.

A reference astrometric solution obtained on a stellar field as described above provides a solid definition of the image orientation and pixel scale that remain constant during the night. However, the origin of the reference frame, i.e. the equatorial coordinates of the image centre, change as the telescope is moved to a new direction in the sky. This means that a new astrometric solution is required for every satellite image. However, these images are taken in non-sidereal mode, as the telescope is set to track the target and not the stars. Any stars passing through the field of view will appear as streaks of light that are about 100 pixels long, based on the image pixel scale of 0.66 arcsec/pix and exposure duration of 5 seconds. Since each star is spread over a relatively long streak, many faint stars are lost in the background noise and cannot be used for the astrometric calibration. This can significantly reduce the number of stars suitable for the calibration, assuming that each streak is detected and processed separately. In order to overcome this difficulty, StarView uses a different algorithm that does not analyse every stellar streak, but rather performs a two-dimensional cross-correlation between a predicted stellar field around the satellite and the actual image. The resulting cross-correlation profile shows a strong elongated peak of the same shape as a bright stellar streak, but including the information from all stars passing through the frame. The centre of the cross-correlation maximum is then measured in pixel units and used to translate the reference astrometric solution obtained on a stellar field, so that the right ascension and declination of the satellite can be obtained. A typical RMS error of this measurement is between 0.2 and 0.3 arcsec. This usually varies during the night as it depends on the satellite brightness and general seeing conditions, as illustrated in Fig. 2. The median values for the night of 20th February were 0.258 arcsec in right ascension and 0.229 arcsec in declination, which correspond to about 40 – 50 m in space at the satellites range of 38,000 km. If we choose to only measure the angular separation between two satellites in the same image, the random uncertainty is further reduced to below 0.1 arcsec, as there is no need to compute a new astrometric solution. Instead, the separation in pixel coordinates can be converted directly to angular units using the pixel scale from the reference stellar field. As an illustration, the median uncertainty for the angular separation on 20th February (Fig. 2) was only about 80 mas, corresponding to about 15 m in space.

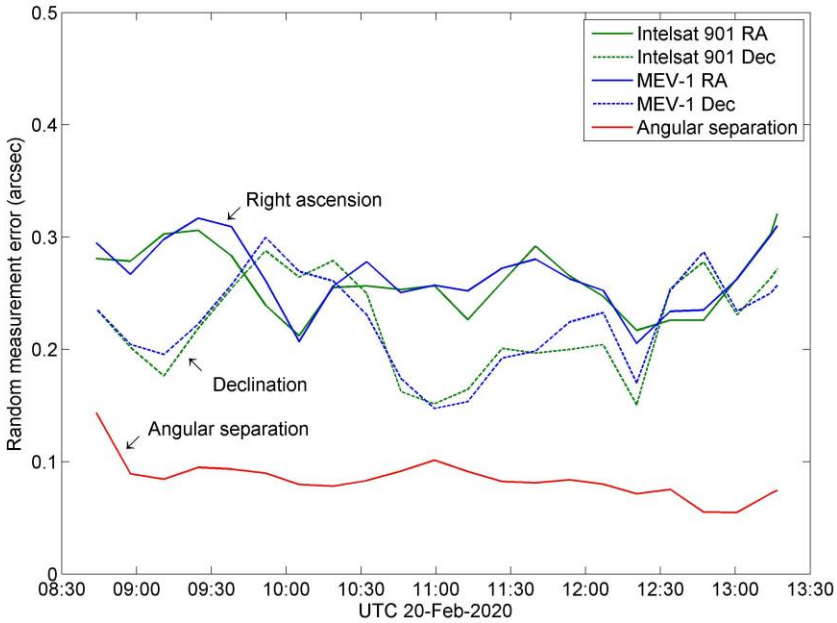

Fig. 2. Astrometric measurement errors

The photometric calibration (brightness scale), on the other hand, is performed on the same reference stellar field by fitting a straight line through the apparent magnitudes (Gaia G-band), as a function of photometric flux on a logarithmic scale. The photometric flux is obtained from the recorded image using standard aperture photometry. The radius of the aperture is adjusted to the width of the PSF (point spread function) and is normally 8 pixels. An additional ring of four pixels around the aperture is used for the estimation of the background scattered light. A linear least-squares fit is then obtained for the stellar magnitude as $m = m_0 - k \log F$, where m_0 is the zero-point of the magnitude scale, k is a linear slope with a theoretical value of 2.5 (from Pogson's law) and F is the integrated photometric flux in ADU (analogue-to-digital units). A typical RMS error of the fit is between 0.1 and 0.2 magnitudes, depending on the number of stars used. However, the random uncertainties in this case are not entirely due to measurement errors. Most of the photometric calibration errors are actually caused by stellar colours (i.e. temperatures), as no astronomical filters are used during our observations. This is acceptable in most studies, as long as we are interested only in detecting relative changes in satellite photometry.

An example of photometric calibration is shown in Fig. 3. The stellar field was centred on a 5-magnitude star HIP 34987 in the constellation of Canis Minor, about 6.5 degrees above the galactic plane, with a total of 462 stars identified down to magnitude 15. Any stars brighter than about 9^m were not included in the photometry, as they appeared saturated in the image after 10 seconds of exposure. About 40 stars (red circles) were rejected from the least-squares fit due to their high residuals (above the 3-sigma level). Those are mainly stars with low photometric fluxes (below 10,000) or stars fainter than magnitude 14. The remaining stars are shown as blue dots. They produce a linear fit with an RMS error of about 0.163 magnitudes. Further investigation showed that the magnitude residuals exhibit a weak correlation with the colour index, as shown in the right panel. This can be taken into account to further reduce the photometric RMS error to below 0.1 magnitudes. However, we do not normally use this option in our photometry, as our observations do not provide any colour information.

Unlike astrometric calibration, which needs to be performed on every satellite image, a single reference photometric calibration can be used throughout the night to measure the brightness of a satellite. The only assumption is that the atmospheric conditions (mainly the transparency of the atmosphere) do not change significantly between the stellar and satellite frames, and that the same photometric aperture is used. The random uncertainty in photometric measurements was typically found between 0.02 and 0.04 magnitudes throughout the night, increasing to about 0.1 for fainter objects (above magnitude 13).

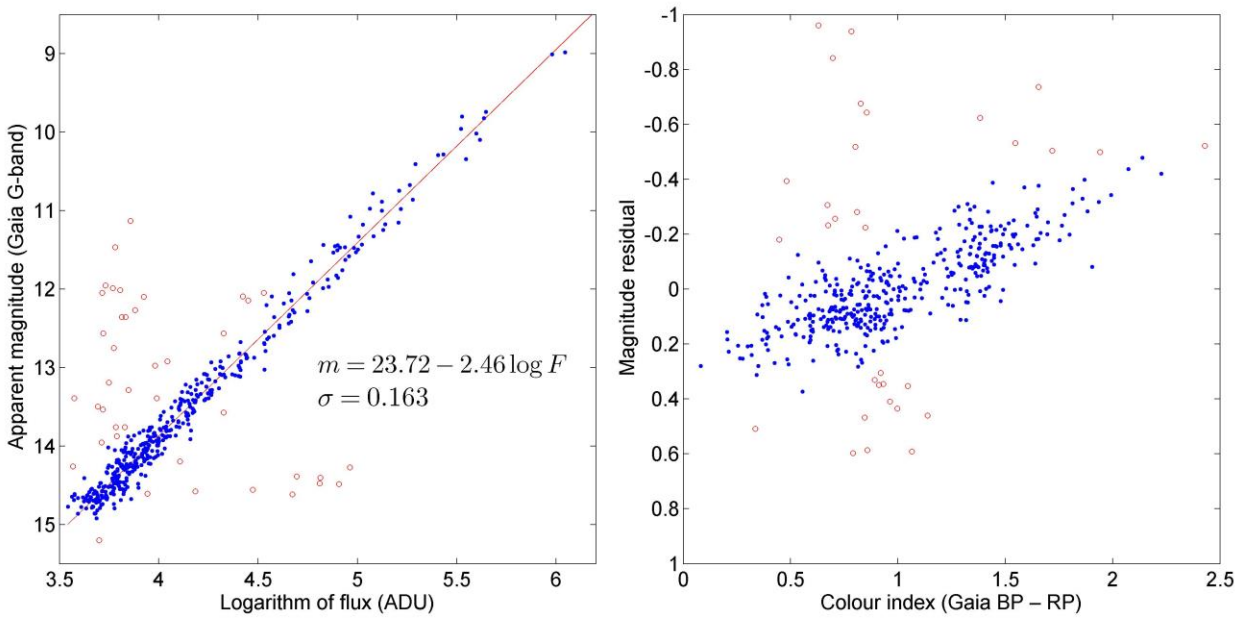

Fig. 3. Photometric calibration

4. RESULTS

A selection of astrometric and photometric measurements of MEV-1 and Intelsat 901 during the docking operation in February 2020 is presented in Figs. 4, 5 and 6. The left panels show the relative astrometry of MEV-1 with respect to Intelsat 901. In this way, many subtle variations in the position are revealed. These changes are not normally seen when the equatorial coordinates are plotted as a function of time, since the right ascension is mainly dominated by the Earth's rotation (15 degrees per hour) and the declination is affected by a considerable north-south drift caused by the orbital inclination (up to several degrees during the night). As the two satellites share the same orbital motion, presenting the astrometry in relative terms has an obvious advantage.

The relative coordinates were calculated using a standard way to project the equatorial coordinates onto the plane of the sky (i.e. perpendicular to the line of sight):

$$\Delta\alpha = \alpha - \alpha_0 \qquad \xi = \Delta\alpha \cos\delta_0$$
$$\Delta\delta = \delta - \delta_0 \qquad \eta = \Delta\delta$$

In these equations, (α, δ) and (α_0, δ_0) are the equatorial positions of MEV-1 and Intelsat 901, respectively, and (ξ, η) are the projected relative coordinates of MEV-1 in arc seconds in the sky. The ξ-axis points to the east (in the direction of increasing right ascension) and the η-axis points to the north. The random errors in relative astrometry were considerably smaller than those obtained for the equatorial coordinates. The median error typically stayed below 0.1 arcsec, or under 20 m in space.

No relative astrometry is shown for the last night of observation on 25th February, as the two satellites already appeared merged into a single object. Most charts showed a relatively smooth orbital motion during each observation night, however there were occasional sudden changes in the direction of motion, as a result of orbital manoeuvring, that are easily seen in the astrometry. For example, a couple of sharp turns just before 11:00 UTC on 11th and 12th February, and also during the final approach before the docking between 13:00 and 14:00 UTC on 24th February.

The photometric light curves are shown in the right panels of Figs. 4 – 6, where the apparent magnitude is plotted as a function of time (UTC). The corresponding equatorial phase angle (as derived from the difference in the right ascensions of the satellites and the Sun) is marked on the top axis. As it is expected for any geostationary satellite,

the light curves in general show a gradual change in brightness during the night, starting with a low value just after sunset and reaching maximum brightness around the zero phase angle, when the satellites were at opposition with the sun. Most of the reflected light from a geostationary satellite comes from the solar arrays. Occasional sharp spikes that were usually seen around the opposition were caused by specular reflection of the sunlight from the polished surfaces. Any other sudden change in brightness was caused by a change in the orientation of the solar arrays during a manoeuvre operation. Several such events can be seen in our photometric data. For example, MEV-1 showed a series of sharp dips and spikes spanning almost four magnitudes (7.5 to 11.3) between about 13:30 and 14:30 UTC on 19th February. Then, on the following night of 20th February, the brightness of MEV-1 was suddenly raised by about half magnitude at 10:25, remained bright for about an hour, and then dropped back to the original brightness. This change was accompanied by sharper spikes on either end. Also interesting to note, the brightness of Intelsat 901 during the entire night of 20th February showed almost continuous variation of about two magnitudes, very untypical for a stable GEO satellite, indicating frequent changes in the satellite attitude.

The last three photometric curves (23rd, 24th and 25th February) also showed a prominent drop in brightness of both satellites caused by a total eclipse, when the two objects entered the Earth's shadow, around 15:00 UTC. During the eclipse, no photometric signature was detected. Also, since an eclipse always happens around the zero phase angle (opposition with the sun), a satellite usually emerges from the shadow with high specular glints. This was recorded in our light curves as very strong spikes of up to magnitude 6 in some cases. The eclipse lasted only 10 minutes on 23rd, but it increased to 20 and 30 minutes on 24th and 25th February, respectively, as the declination of the two satellites changed around the opposition.

Multiple changes in the brightness of both MEV-1 and Intelsat 901 were observed on 24th February before and after the eclipse, as the two satellites were preparing for docking. The brightness of MEV-1 dropped by about a magnitude for half an hour between 13:00 and 14:00 UTC. Soon after that, there was a sudden drop in the brightness of Intelsat 901, about one hour before the eclipse. After the eclipse, MEV-1 continued with a series of sharp changes, but the observations had to be stopped at this point due to increased sky brightness at dawn.

5. SUMMARY

Astrometric and photometric measurements of Mission Extension Vehicle 1 (MEV-1) and Intelsat 901 were obtained from New Zealand during the docking operation between the two satellites in February 2020. The observations were collected using the 11-inch (279-mm) f/10 Cassegrain telescope of the Defence Technology Agency's SDA Observatory at Whangaparaoa, near Auckland. An FLI ML 11002 full-frame CCD camera was used as a detector, providing a pixel scale of about 0.66 arcsec/pix and a diagonal field of view of just under one degree. Over 11,000 images were collected during 11 nights of observation. The two satellites were last recorded at a separation of 2.8 arcsec (about 500 m) during their final approach on 24th February.

The data reduction was performed using StarView, a dedicated SDA image analysis tool developed at DTA. The astrometric and photometric calibration was based on Gaia DR2 catalogue using over 70 million stars down to magnitude 16. Typical calibration uncertainty was between 0.1 and 0.2 arcsec in astrometry, and 0.1 to 0.2 magnitudes in photometry. The random measurement errors were much smaller, typically less than 0.1 arcsec in astrometry and 0.1 magnitudes in photometry. Combined with a sampling rate of about 3 frames per minute, this has enabled detection of small changes in position and brightness of the two satellites.

Both astrometric and photometric measurements showed numerous characteristic features resulting from orbital manoeuvring and attitude changes of the two satellites during the rendezvous operations. This work has demonstrated that readily available small-aperture optical equipment can successfully be used to monitor proximity operations in the GEO regime and to collect important information for space domain awareness.

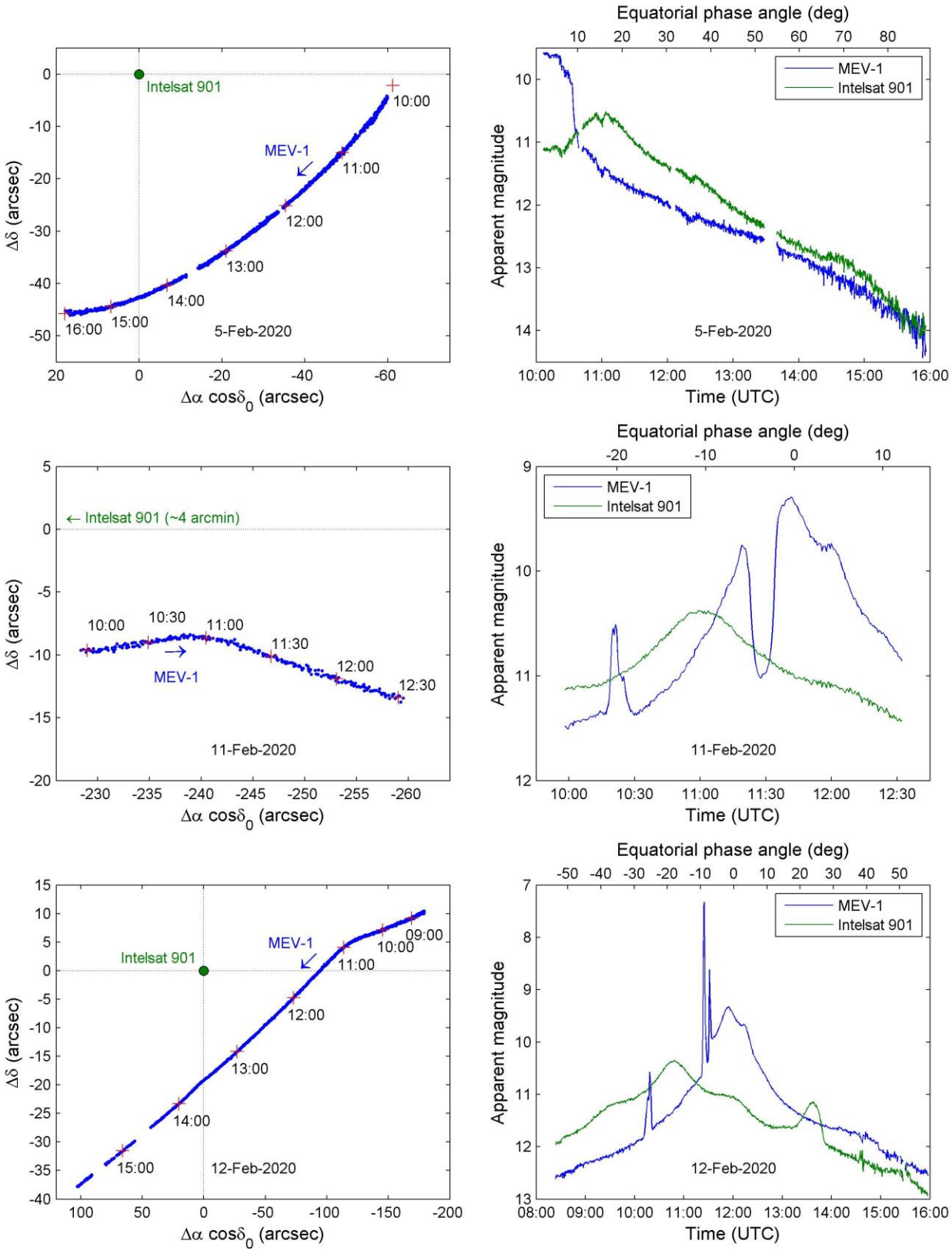

Fig. 4. Relative astrometry and photometric light curves of Intelsat 901 and MEV-1 (Part I)

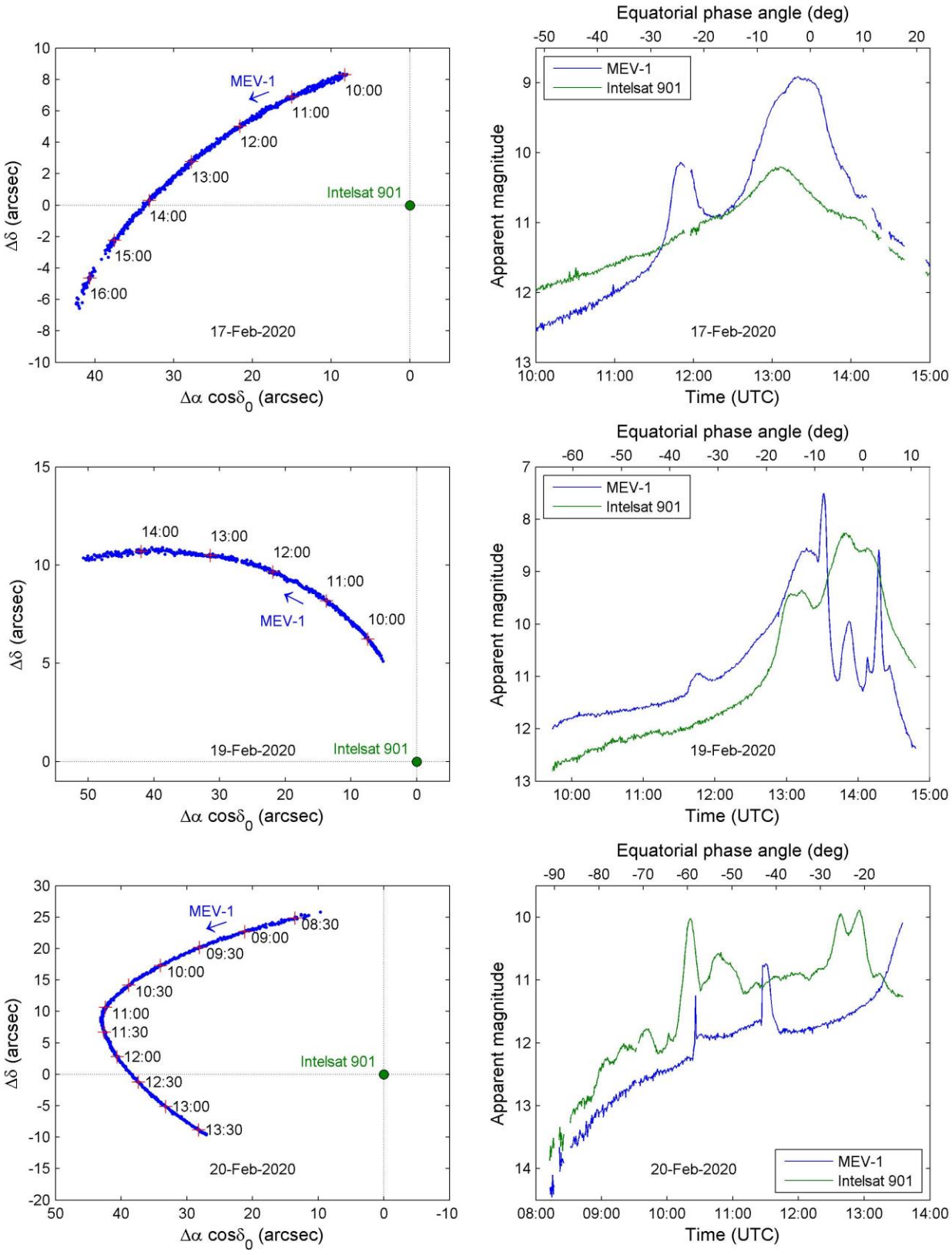

Fig. 5. Relative astrometry and photometric light curves of Intelsat 901 and MEV-1 (Part II)

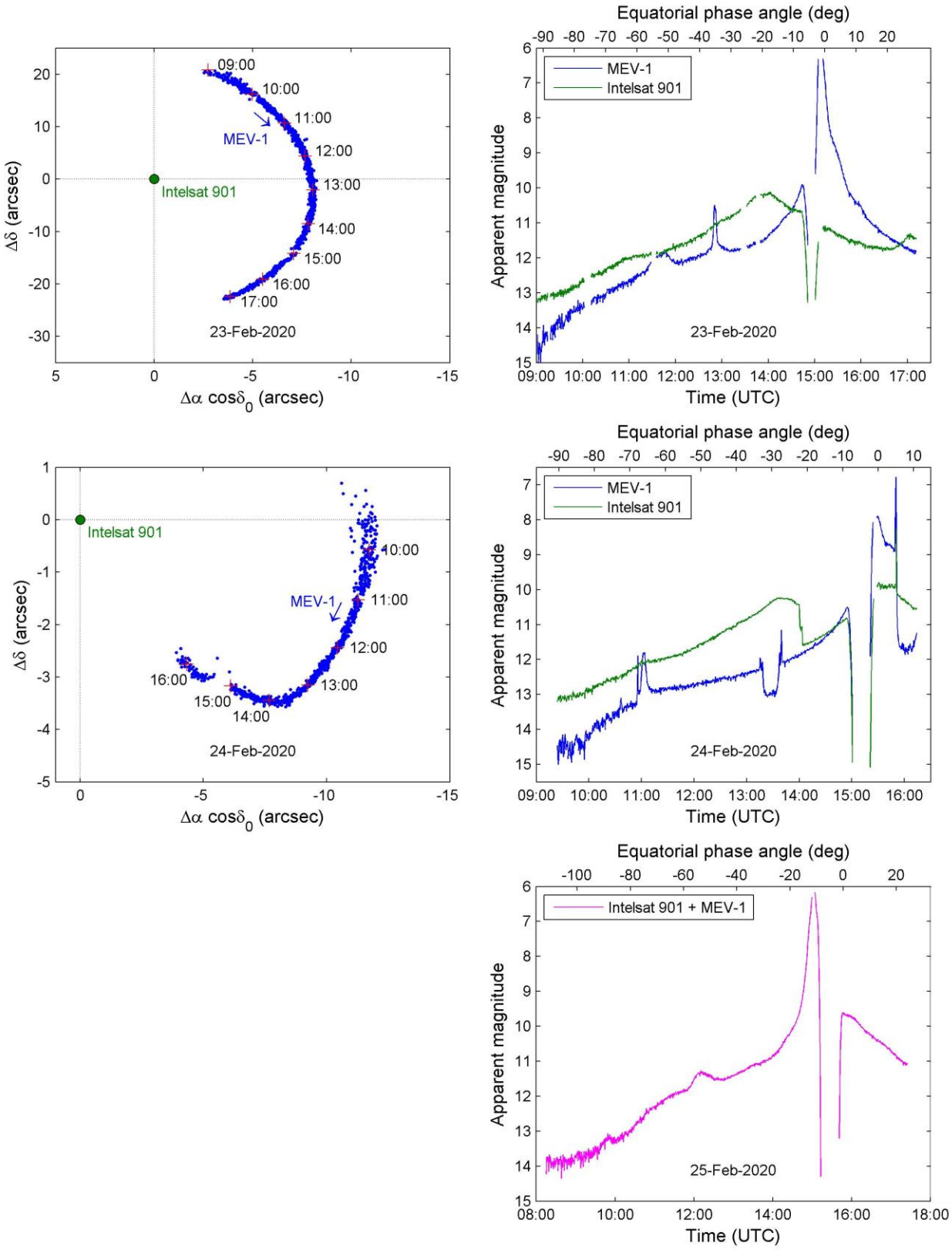

Fig. 6. Relative astrometry and photometric light curves of Intelsat 901 and MEV-1 (Part III)

6. REFERENCES

[1] S. George, A. Ash. T. Bessell, L. Scott, J. Skuljan, J. Frith, R. Furfaro, V. Reddy. Phantom Echoes: A Five-Eyes SDA Experiment to Examine GEO Rendezvous and Proximity, *Proc 21st AMOS Conf.,* 2020

[2] J. Skuljan and J. Kay. Automated astrometric analysis of satellite observations using wide-field imaging, *Proc. 17th AMOS Conf.,* pp. 240-249, 2016

[3] J. Skuljan. QuadCam – a quadruple polarimetric camera for space situational awareness, *Proc. 18th AMOS Conf.,* pp. 275-285, 2017

[4] J. Skuljan. Photometric measurements of geostationary satellites over the Western Pacific Region, *Proc. 19th AMOS Conf.,* pp. 1420-1428, 2018

[5] Gaia Collaboration, Prusti, T., de Bruijne, J. H. J., Brown, A. G. A., Vallenari, A., Babusiaux, C., Bailer-Jones, C. A. L., Bastian, U., Biermann, M., Evans, D. W., et al. The Gaia mission, *A&A, 595,* pp. A1, 2016

[6] Gaia Collaboration, Brown, A. G. A., Vallenari, A., Prusti, T., de Bruijne, J. H. J., Babusiaux, C. and Bailer-Jones, C. A. L. Gaia Data Release 2. Summary of the contents and survey properties, *ArXiv e-prints,* 2018